

Original paper

Diagnostic accuracy of an integrated approach using conventional ultrasonography, and Doppler and strain elastography in the evaluation of superficial soft tissue lesions

Abhiman Baloji^{B,C,D,F}, Ranjan Chandra^{A,E,F}, Neha Bagri^{A,D,E,F}, Ritu Misra^{E,F}, Rajni K^B, Sharathkumar S Prabhu^{C,F}

Vardhman Mahavir Medical College and Safdarjung Hospital, New Delhi, India

Abstract

Purpose: To assess the diagnostic accuracy of an integrated approach using conventional ultrasonography, colour Doppler ultrasonography, and elastography strain ratios in tandem in the evaluation of superficial soft tissue lesions.

Material and methods: Sixty-five subjects were included in this prospective cross-sectional study. Greyscale features and Doppler parameters were recorded. Strain elastography of the non-vascular and non-cystic lesions was performed and strain ratios were calculated. Fine-needle aspiration or biopsy of all the lesions was performed depending on their site and condition. Inter-rater k agreement was used to determine the strength of agreement between imaging-based diagnosis and histopathological diagnosis. A diagnostic test was used to calculate the sensitivity, specificity, positive predictive value, and negative predictive value. A p value of < 0.05 was considered statistically significant.

Results: Multiple superficial soft tissue lesions were studied, the majority of which were lipomas, vascular anomalies, and epidermoid cysts. The diagnostic accuracy was very high and varied from 92.31% to 100% for various masses. The imaging-based diagnosis was in agreement with the histopathological diagnosis in 86.15% ($n = 56$) and disagreement in 13.85% ($n = 9$) of the cases ($p < 0.007$). There was very good inter-rater agreement between the imaging-based diagnosis and histopathological diagnosis ($\kappa = 0.818$).

Conclusions: The combined use of conventional ultrasonography, colour Doppler, and elastography strain ratios provides a very effective non-invasive tool for the diagnosis of superficial soft tissue lesions and may negate the need for unnecessary biopsies. The advantage of this integrated approach using various ultrasound techniques needs no further emphasis.

Key words: ultrasonography, soft tissue, Doppler, strain ratio.

Introduction

Superficial soft tissue masses are a common clinical entity in our day-to-day practice. Skin covers the entire external surface of the body, and the musculoskeletal framework constitutes 8% of the total body mass [1]. Skin is divided into the superficial epidermis and the deeper dermis. The epidermis is a derivative of the surface ectoderm, and the dermis arises from somatopleuric mesoderm. The sub-

cutaneous tissue is a milieu of fat, collagen fibres, elastin fibres, blood vessels, etc. covering the musculoskeletal framework of the body. Due to the presence of the myriad types of cells in the skin and subcutaneous tissue, there are a lot of lesions arising from the various cells.

The World Health Organization (WHO) has classified soft tissue masses based on the type of cell of origin into various groups, such as adipocytic, fibroblastic, fibrohistiocytic-like, vascular, pericytic, skeletal muscle, smooth

Correspondence address:

Dr. Neha Bagri, Department of Radiodiagnosis, Vardhman Mahavir Medical College and Safdarjung Hospital, 110029, New Delhi, India, phone: 09013606279, e-mail: drnehabagri@gmail.com

Authors' contribution:

A Study design · B Data collection · C Statistical analysis · D Data interpretation · E Manuscript preparation · F Literature search · G Funds collection

Table 1. WHO classification of soft tissue tumours

Adipocytic tumours
Fibroblastic/myofibroblastic tumours
So-called fibrohistiocytic tumours
Smooth muscle tumours
Pericytic (perivascular) tumours
Skeletal tumours
Vascular tumours
Chondro-osseous tumours
Gastrointestinal stromal tumours
Nerve sheath tumours
Tumours of uncertain differentiation
Undifferentiated/unclassified tumours

Table 2. Sonographic appearance of normal soft tissue and osseous structures

Soft tissue and osseous structures	Sonographic appearance
Epidermis, dermis	Hyperechoic
Hypodermis	Hypoechoic fat and hyperechoic fibrous septations
Tendon	Hyperechoic with fibrillary echotexture
Muscle	Hypoechoic
Bone and calcium	Hyperechoic with posterior acoustic shadowing
Fibrocartilage	Hyperechoic
Ligaments	Hyperechoic; striations more compact than with tendon
Peripheral nerve	Fascicular; nerve fascicles hypoechoic surrounded by hyperechoic connective tissue
Lymph node	Reniform hypoechoic structure with central echogenicity

muscle, chondrosseous, gastrointestinal stromal tumours (GIST), and nerve sheath lesions (Table 1). The annual clinical incidence of benign soft tissue tumours has been estimated at up to 3000 per million population, and they outnumber their malignant counterparts by 100 fold. At least one-third of the soft tissue tumours are lipomas, one-third fibrohistiocytic and fibrous tumours, 10% vascular tumours, and 5% nerve sheath tumours [2].

The treatment and prognosis of subcutaneous soft-tissue lesions largely depends on the histologic type and extent. Recognition of a specific tumour type on ultrasound enhances its management and helps to make a decision about the need for percutaneous biopsy or additional imaging such as magnetic resonance imaging (MRI). The sonographic appearance of normal soft tissue structures was described by Jacobson in 2007 and helps determine the site of origin of the mass (Table 2) [3]. Several imaging modalities have been used to assess soft-tissue

lesions, including plain radiography, various ultrasound techniques like conventional ultrasonography (USG), colour Doppler ultrasonography (CDU), and elastography strain ratios (ESR) in combination or in isolation, computed tomography (CT), MRI, angiography, nuclear medicine, and positron emission tomography (PET). High-resolution USG and Doppler are being used as the first line of investigation to evaluate these superficial soft-tissue lesions. The benefits of ultrasonography include ready and easy applicability, availability, relatively low cost, higher accuracy in differentiating tissue layers, good spatial and contrast resolution, as well as real-time imaging capability. However, it has its own inherent disadvantages because it is an operator-dependent modality demanding a certain level of experience from the examiner. Elastography, a newer advancement of imaging, is a novel technique giving information regarding tissue elasticity. Mapping the stiffness can either be estimated from the analysis of the strain in the tissue under stress (quasi-static methods) or by the imaging of shear waves whose propagation is governed by the tissue stiffness [4]. In strain elastography, stress is applied by repeated manual compression of the transducer, and the amount of lesion deformation relative to the surrounding normal tissue is measured and displayed in colour. Strain elastography involves deformation of the tissue followed by imaging of the degree of compression or extension of the tissue [5].

Many studies in the recent past have been conducted with the use of conventional ultrasonography, colour Doppler, and elastography in isolation or combination. However, studies with an integrated approach employing all the three techniques simultaneously are lacking.

Histopathological examination continues to be the gold standard for the diagnosis of soft tissue lesions. However, it is invasive and thus comes with inherent risks like pain, bleeding, wound infection, and even the rarer possibility of spreading a malignant tumour via seeding [6]. Thus, there is a paradigm shift to imaging-based diagnosis of soft tissue lesions.

Material and methods

We prospectively included 65 subjects presenting with superficial soft tissue lesions to our institute between November 2017 and April 2019. The study subjects comprised 39 male and 26 female subjects, aged between 3 and 67 years (mean age: 36 ± 8 years). The lesions with deep/intramuscular component and subjects having history of prior intervention/ biopsy of the tumour were excluded from the study.

Imaging procedure

An integrated approach using various ultrasound techniques (greyscale, colour Doppler, and elastography) were performed simultaneously in each case. Conventional

ultrasonography was performed following standardised protocols using linear array transducers of frequency 5-17 MHz and 3-9 MHz, and the parameters recorded were location, number, size, shape, echogenicity, and margins for each superficial lesion. Doppler assessment was also done to evaluate the presence or absence of vascularity, pattern of vascularity – whether peripheral or central, and the Doppler parameters (resistivity index, pulsatility index) of the lesions.

Subsequently, elastography was performed in the non-cystic and non-vascular lesions using a linear array transducer of frequency between 5 and 17 MHz with same depth focus and gain settings as for conventional ultrasonography, and the size/strain ratios were determined. Elastography could be performed only in 48 lesions because the rest of the lesions were either cystic or vascular lesions in which elastography was not possible.

All of the cases evaluated by ultrasonography were subjected to pathological examination in the form of FNAC/biopsy. Before the procedure, all patients were questioned for contraindications such as anticoagulant treatment or anxiety that could interfere with the biopsy. After the histopathological results were obtained, the final pathological diagnosis was compared with the imaging-based diagnosis.

Statistical analysis

Statistical Package for Social Sciences (SPSS) version 21.0 was used for analysis. Inter-rater k agreement was used to find out the strength of agreement between imaging-based diagnosis and histopathological diagnosis. A diagnostic test was used to calculate sensitivity, specificity, positive predictive value (PPV), and negative predictive value (NPV). A *p* value of < 0.05 was considered statistically significant.

Ethical statement

This study was approved by our institute’s Research Ethics Committee (IEC/VMMC/SJH/S. No. 183), and written, informed consent was taken from all the subjects prior to enrolment. All procedures performed in studies involving human participants were in accordance with the ethical standards of the institution and the national research committee, and with the 1964 Helsinki declaration and its later amendments or comparable ethical standards.

Results

The superficial soft tissue lesions comprised 26 lipomas, including the following: 13 vascular anomalies, nine epidermoid cysts, four neurofibromas, two each of lymph nodes, branchial cysts, fibromas, endometriomas, and one each of schwannoma, fibrohistiocytic lesion, chronic expanding haematoma, and schwannoma with cavernous

malformation and metastases. Most of the lesions (66%) were located in the upper limb and neck region.

Lipomas, constituting the majority of lesions, were predominantly hyperechoic on conventional ultrasonography, and rest of the lesions were majorly heteroechoic. Doppler assessment was performed to look for the pattern of vascularity and further characteristic parameters, including resistive and pulsatility indices (Figures 1 and 2).

Subsequently, strain elastography was performed to evaluate the size ratio (Figure 3) and strain ratio. Elastography could be performed in 48 lesions; the rest of the lesions were either cystic or vascular in nature. Of these 48 lesions the strain ratio was calculated in all, whereas the size ratio could not be evaluated in 10 lesions due to their larger size in comparison to the probe. The average strain ratio of the lesions in this series was 1.72 ± 0.94 with a wide variability amongst the different pathologies (Figure 4).

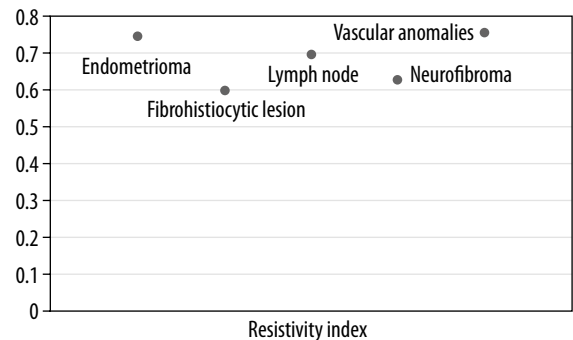


Figure 1. Mean resistivity index values of vascular lesions

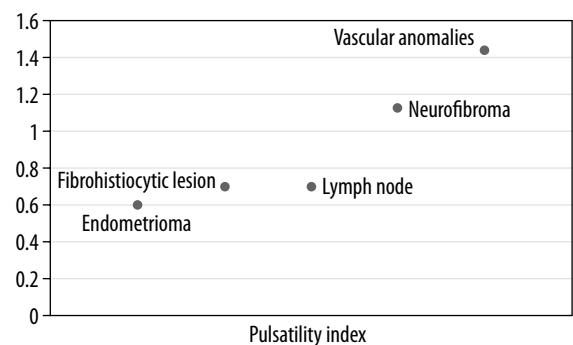


Figure 2. Mean pulsatility index values of vascular lesions

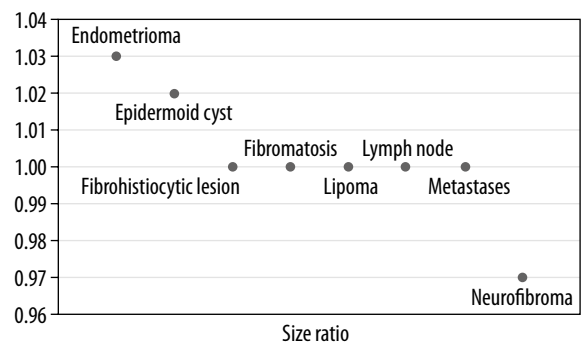


Figure 3. Mean size-ratio of the lesions

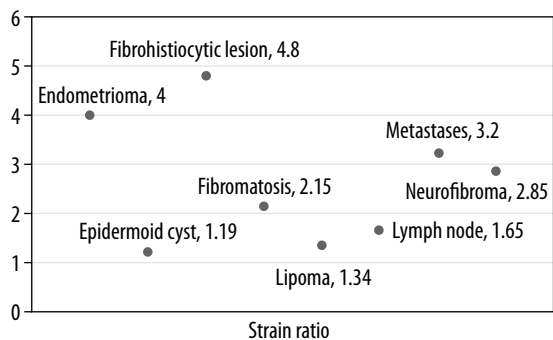


Figure 4. Mean strain-ratio of the lesions

Table 4. Specificity of integrated approach in the evaluation of superficial soft tissue masses

Histopathological diagnosis	Specificity (%)
Epidermoid cyst	98.18
Endometrioma	98.44
Lipoma	94.74
Fibromatosis	98.44
Vascular anomalies	100.00
Neurofibroma	98.33
Branchial cyst	100.00
Lymph node	100.00
Metastases	100.00
Schwannoma	98.46
Chronic expanding haematoma	100.00

The sensitivity and specificity of this integrated diagnostic approach in the evaluation of various superficial soft tissue lesions varied from 80% to 100% (Table 3) and from 95% to 100% (Table 4), respectively. The positive and negative predictive values of this integrated approach were

Table 3. Sensitivity of integrated approach in the evaluation of superficial soft tissue lesions

Histopathological diagnosis	Sensitivity (%)
Epidermoid cyst	80.00
Endometrioma	100.00
Lipoma	88.89
Fibromatosis	100.00
Vascular anomalies	92.86
Neurofibroma	60.00
Branchial cyst	100.00
Lymph node	100.00
Metastases	100.00
Chronic expanding haematoma	100.00

also determined considering the histopathology of superficial soft tissue masses as the gold standard (Table 5).

The diagnostic accuracy of an integrated diagnostic approach was very high and varied from 92.31% to 100% for various lesions (Table 6). The imaging-based diagnosis was in agreement with the histopathological diagnosis in 86.15% ($n = 56$) and disagreement in 13.85% ($n = 9$) of the cases ($p < 0.007$). There was very good inter-rater agreement between the imaging-based diagnoses and histopathological diagnoses ($\kappa = 0.818$).

Discussion

Lesions that can present in the superficial planes can be myriad, and imaging plays a vital role in their characterisation and diagnosis. The utility of multiple ultrasound techniques used simultaneously may add to the diagnostic accuracy of superficial soft tissue lesions.

Table 5. Positive and negative predictive values of Integrated approach in the evaluation of superficial soft tissue masses

Histopathological diagnosis	Positive predictive value (%)	Negative predictive value (%)
Epidermoid cyst (95% CI)	88.89 (51.75–99.72)	96.43 (87.69–99.56)
Endometrioma (95% CI)	50.00 (1.26–98.74)	100.00 (94.31–100.00)
Lipoma (95% CI)	92.31 (74.87–99.05)	92.31 (79.13–98.38)
Fibromatosis (95% CI)	50.00 (1.26–98.74)	100.00 (94.31–100.00)
Vascular anomalies (95% CI)	100.00 (75.29–100.00)	98.08 (89.74–99.95)
Neurofibroma (95% CI)	75.00 (19.41–99.37)	96.72 (88.65–99.60)
Fibrohistiocytic lesion (95% CI)	0.00 (0.00–97.50)	100.00 (94.40–100.00)
Branchial cyst (95% CI)	100.00 (15.81–100.00)	100.00 (94.31–100.00)
Lymph node (95% CI)	100.00 (15.81–100.00)	100.00 (94.31–100.00)
Schwannoma with cavernous haemangioma (95% CI)	0.00 (0.00–97.50)	100.00 (94.40–100.00)
Metastases (95% CI)	100.00 (2.50–100.00)	100.00 (94.40–100.00)
Schwannoma (95% CI)	0.00 (0.00–97.50)	100.00 (94.40–100.00)
Chronic expanding haematoma (95% CI)	100.00 (2.50–100.00)	100.00 (94.40–100.00)

Table 6. Diagnostic accuracy of integrated approach to superficial soft tissue masses

Histopathological diagnosis	Diagnostic accuracy (%)
Epidermoid cyst (95% CI)	95.38
Endometrioma (95% CI)	98.46
Lipoma (95% CI)	92.31
Fibromatosis (95% CI)	98.46
Vascular anomalies (95% CI)	98.46
Neurofibroma (95% CI)	95.38
Fibrohistiocytic lesion (95% CI)	98.46
Branchial cyst (95% CI)	100.00
Lymph node (95% CI)	100.00
Schwannoma with cavernous haemangioma (95% CI)	98.46
Metastases (95% CI)	100.00
Schwannoma (95% CI)	98.46
Chronic expanding haematoma (95% CI)	100.00

Lipomas constituted the larger part (40%) of the lesions evaluated in this study, and they were quite variable in their appearance, similar to that reported by Fornage *et al.* [7]. We found that the majority of the lipomas (73%) were hyperechoic (Figure 5). Only two (7.7%) lipomas were hypoechoic, while the rest (19.23%) were heteroechoic. Despite their variable appearance on greyscale images, the sensitivity and specificity for the diagnosis of lipomas utilising an integrated approach stood at 88.89% and 94.74%, respectively. In the systematic review of diagnostic accuracy of ultrasound for soft tissue lipomas by Rahmani *et al.* the sensitivity and specificity were 86.87% and 95.95%, respectively, concordant with our study [8].

Our results for evaluation of lipomas were also comparable to the study conducted by Hung *et al.*, who reported

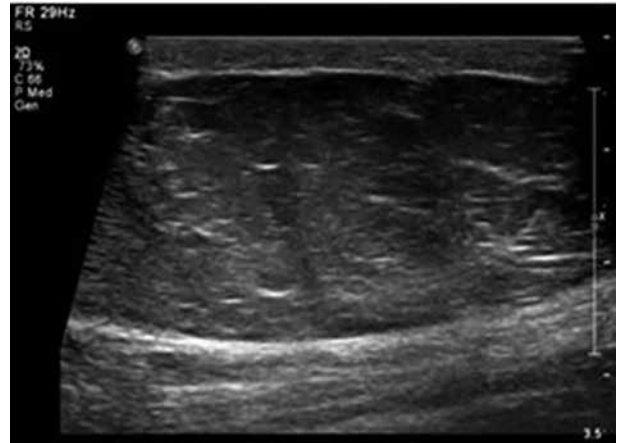


Figure 5. Lipoma – greyscale ultrasound image shows a large, well-defined hyperechoic lesion with few linear echogenic foci within in the subcutaneous plane

a sensitivity of 95.2% and specificity of 94.3%; however, they incorporated only conventional ultrasonography [9].

The use of an integrated diagnostic approach in our study raised the diagnostic accuracy for superficial lipomas to 92.31% as compared to the study by Inampudi *et al.*, in which they retrospectively analysed superficial and deep soft tissue lipomas using conventional ultrasonography alone and reported a sensitivity ranging from 40% to 52% and specificity 64% to 86% [10]. Whether the higher diagnostic accuracy can be attributed to the integrated approach employed in our study or the selection criteria of subjects and methodology used needs to be investigated by further studies.

Epidermoid cysts can occasionally mimic lipomas clinically. Although the presence of a black punctum at the summit of the lesion usually suffices to diagnose the entity, it is not very frequent. They appear as well-defined, predominantly hypoechoic lesion showing posterior acoustic enhancement on ultrasound (Figure 6). The sensitivity and specificity of the integrated approach in the diagnosis of epidermoid cysts were 80.00% and 98.18%,

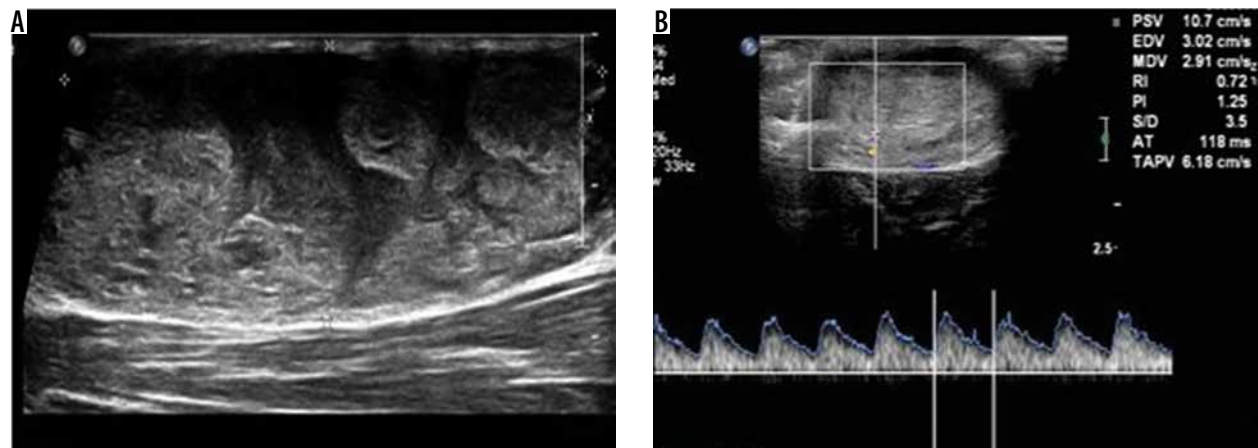


Figure 6. Epidermoid cyst – greyscale ultrasound image (A) shows a well-defined, predominantly hypoechoic lesion with posterior acoustic enhancement. Strain elastography assessment (B) of the same lesion depicts it predominantly in blue colour on elastography map and a strain ratio of 1.03 suggesting the “soft” nature of the lesion and a pointer towards a benign aetiology

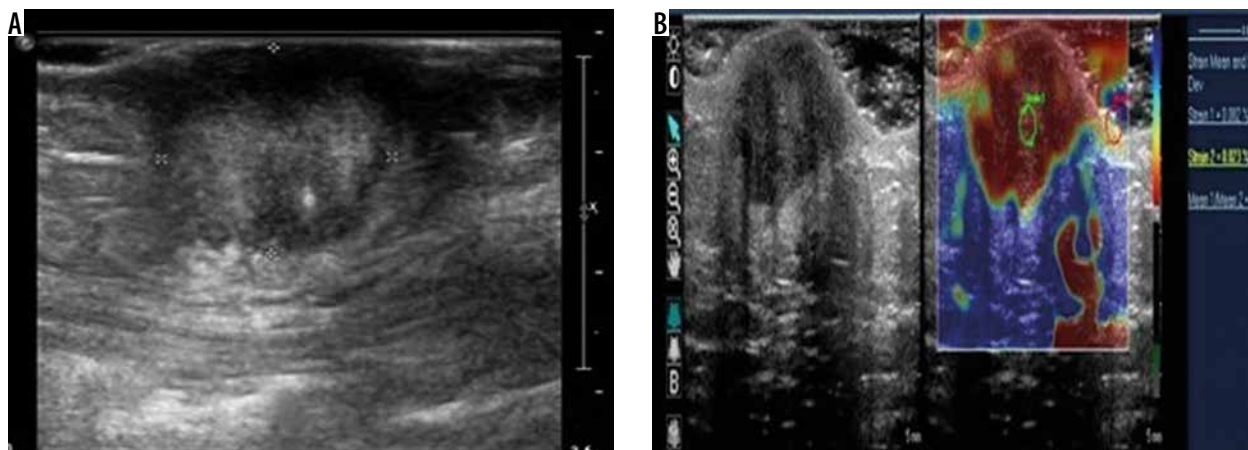


Figure 7. Schwannoma with cavernous malformation – greyscale ultrasound image (A) shows a well-defined heterogeneously hyperechoic lesion. Spectral Doppler image (B) of the same lesion shows internal vascularity with arterial waveform

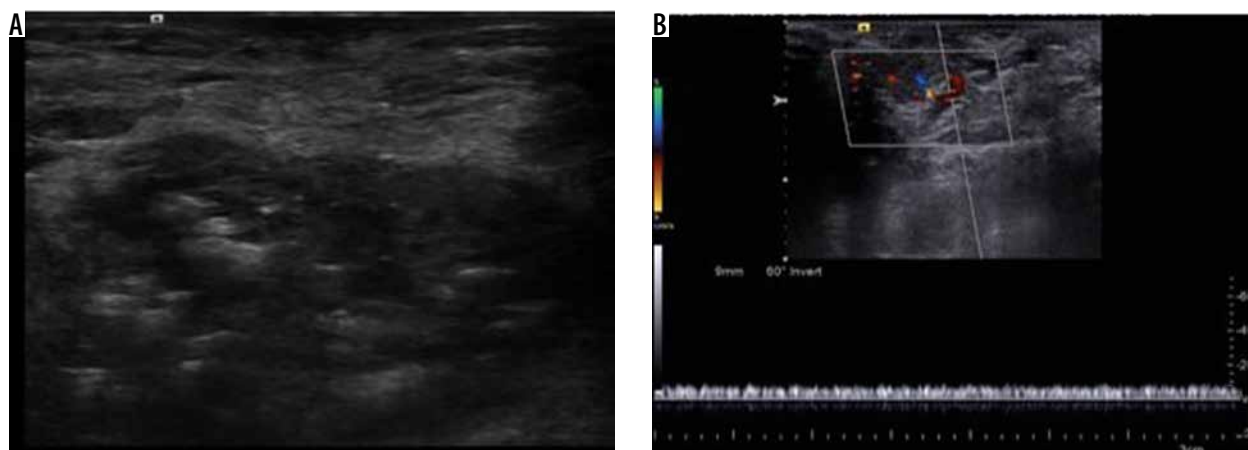


Figure 8. Anterior abdominal wall endometrioma – greyscale ultrasound image (A) shows a well-defined, round, hyperechoic lesion seen in the subcutaneous plane. Strain elastography (B) of the same lesion depicts it predominantly in red colour on an elastography map and a strain ratio of 3.57 suggesting the “hard” nature of the lesion. However, the lesion turned out to be endometrioma on histopathology

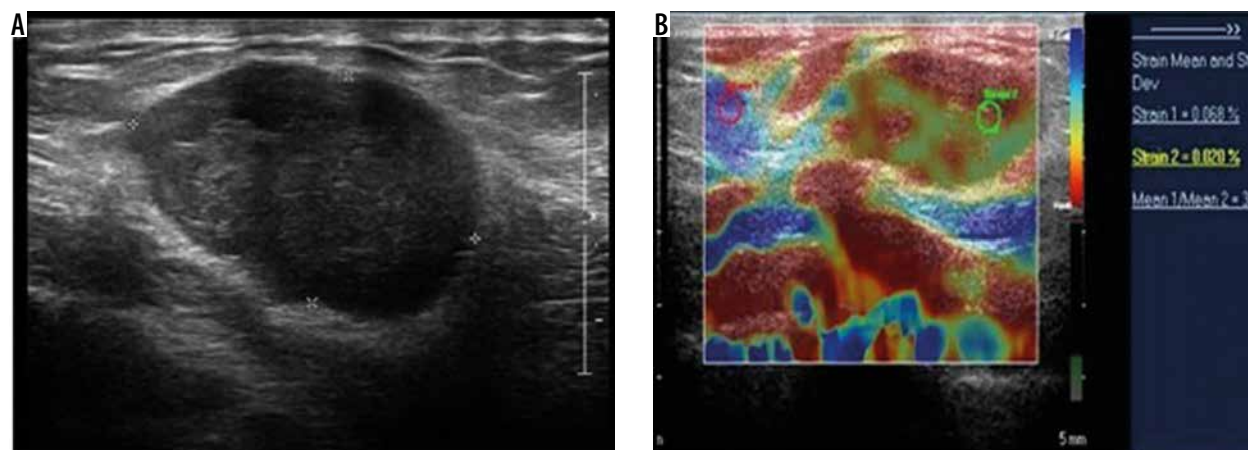


Figure 9. Haemangioma – greyscale ultrasound image (A) shows a well-defined hypoechoic lesion with hyperechoic foci associated with posterior acoustic shadowing. Colour and spectral Doppler examination (B) of the same lesion demonstrates venous flow within the lesion. The findings were suggestive of haemangioma

respectively. The sensitivity and specificity for the diagnosis of epidermoid cyst using routine greyscale ultrasound alone was found to be 65.9% and 99.3%, respectively, by Kuwano *et al.* in a series of 183 patients, which included

44 epidermoid cysts [11]. Although the specificity of our study and of the study by Kuwano *et al.* does not show any significant difference, the disparity in sensitivity can probably be attributed to a larger sample size in the study

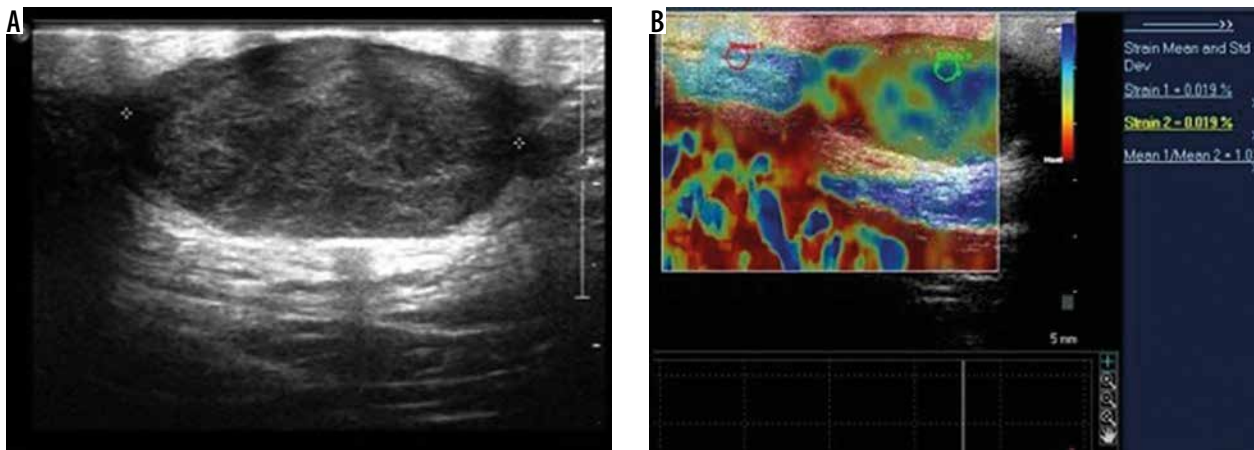


Figure 10. Subcutaneous metastases – greyscale ultrasound image (A) shows a well-defined hypoechoic lesion in the subcutaneous plane of anterior chest wall. Strain elastography (B) of the same lesion depicts it predominantly in red colour on an elastography map and a strain ratio of 3.45 suggesting the “hard” nature of the lesion and a pointer towards a malignant aetiology

by Kuwano and the use of strain elastography as an extra modality in our study.

These results in the context of epidermoid cysts in the present study are also comparable to the study of superficial soft tissue masses by Hung *et al.* [9]. The “pseudotestis” appearance of epidermoid cysts was extensively studied by Huang *et al.* in a retrospective study of 42 surgically proven cases [12]. The pseudotestis appearance is characterised by an ovoid nodule with homogeneous echoes within.

The mean strain ratio in epidermoid cysts was 1.19 ± 0.08 , which overlapped with that of lipomas (1.34 ± 0.45). The retrospective study by Park *et al.* found no significant differences between the strain elastography scores of epidermoid cysts and that of other benign tumours [13]. However, the epidermoid cysts were softer than the malignant superficial tumours. Although our study had limited number of cases, the single subcutaneous metastatic lesion we encountered had a strain ratio of 3.2 and that of fibroma and neurofibroma was higher than that of epidermoid cyst at 2.15 ± 0.92 and 2.85 ± 0.54 , respectively. However, the significance of this could not be ascertained because it was a single case.

Six peripheral nerve sheath tumours were encountered in this study, of which four were neurofibromas, one schwannoma, and another schwannoma with cavernous haemangioma (Figure 7). The presence of peripheral nerve continuity and internal blood flow are pointers to the diagnosis of peripheral nerve sheath tumour. Although the imaging appearances of neurofibroma and schwannoma are identical, the presence of an eccentrically entering nerve is a pointer towards schwannoma [14]. However, ultrasound alone was poor in distinguishing neurofibroma from schwannoma [15]. Of the four neurofibromas in this series, entering/exiting nerve was seen in three of the lesions, all of which demonstrated a central relationship to the lesion, as described by Ryu *et al.* [16]. The average maximum size of the neurofibroma (2.78 ± 0.33) was higher than the maximum diameter of the schwannoma (1.1 ± 0).

Abdominal wall endometriomas are a rare occurrence, and their incidence varies between 0.03% and 1% [17,18]. They usually occur in the region of an abdominal scar following previous caesarean section, hysterotomy, etc. We encountered two subcutaneous anterior abdominal wall endometriomas, of which one was heteroechoic and the other was hyperechoic (Figure 8). A single peripheral twig of vascularity as described by Francica was demonstrated in one of the lesions [19]. Although twinkling artefact was claimed to be a specific ancillary finding in superficial endometriomas by Clarke *et al.*, we could not demonstrate this in either of the lesions we came across [20].

A total of 13 vascular anomalies were included, of which seven were haemangiomas and six were vascular malformations. Colour Doppler study has always been the first line of investigation in the evaluation of vascular lesions. The haemangiomas demonstrated phleboliths within and all but one lesion demonstrated some form of vascularity (Figure 9). The vascular malformations included in this study encompassed capillary, venous, and arteriovenous types.

During the duration of this study, we came across a single malignant superficial lesion in the form of a cutaneous metastatic lesion located in the anterior chest wall in a known case of melanoma of the foot (Figure 10). The lesion was hypoechoic and demonstrated a strain ratio of 3.2 on strain elastography. Li *et al.* found an average strain ratio value of 5.42 ± 3.47 in malignant soft tissue masses, which was higher than that found in benign lesions (1.80 ± 2.10) [21]. Strain ratio > 2.295 and elastic score > 3 was found to be highly sensitive for diagnosing malignant soft tissue tumours (93.8 and 100%, respectively), but the specificity was poor (80.5 and 51.6%, respectively) [21]. However, because we encountered a single case of cutaneous metastatic lesion, calculating the sensitivity and specificity in this context is a limitation of the present study.

Tavare *et al.* summarised in their prospective study of 206 consecutive cases that the accuracy of soft-tissue mass diagnosis can be increased by combining B-mode

ultrasonography with shear wave elastography. They further stated that although the diagnostic accuracy was increased, a single cut-off would not be acceptable on account of differences in the location of the lesion and the age of the patient [22].

Conclusions

An integrated approach in the evaluation of superficial soft tissue masses with various ultrasound techniques

had a statistically high degree of accuracy (k value 0.818) and can enhance the diagnostic accuracy and may negate the need for histopathological examination in many cases.

Conflict of interest

The authors report no conflict of interest.

References

1. Wigley C. Skin and its appendages. In: Gray's Anatomy. The Anatomical Basis of Clinical Practice. 40th ed. Standring S (ed.). Elsevier, 2008; 145.
2. Fletcher CD, Hogendoorn P, Mertens F, Bridge J. WHO Classification of Tumours of Soft Tissue and Bone. 4th ed. IARC Press, Lyon 2013.
3. Jacobson JA. Fundamentals of musculoskeletal ultrasound. 1st ed. Saunders Elsevier, Philadelphia 2007; 1.e5-6.
4. Gennison JL, Deffieux T, Fink M, Tanter M. Ultrasound elastography: principles and techniques. *Diagn Interv Imaging* 2013; 94: 487-495.
5. Chang JM, Won JK, Lee KB, Park IA, Yi A, Moon WK. Comparison of shear-wave and strain ultrasound elastography in the differentiation of benign and malignant breast lesions. *Am J Roentgenol* 2013; 201: 347-356.
6. Shyamala K, Girish HC, Murgod S. Risk of tumor cell seeding through biopsy and aspiration cytology. *J Int Soc Prevent Commun Dent* 2014; 4: 5-11.
7. Fornage BD, Tassin GB. Sonographic appearances of superficial soft tissue lipomas. *J Clin Ultrasound* 1991; 19: 215-220.
8. Rahmani G, McCarthy P, Bergin D. The diagnostic accuracy of ultrasonography for soft tissue lipomas: a systematic review. *Acta Radiol Open* 2017; 6: 2058460117716704.
9. Hung EHY, Griffith JE, Ng AWH, Lee RKL, Lau DTY, Leung JCS. Ultrasound of musculoskeletal soft tissue tumours superficial to the investing fascia. *Am J Roentgenol* 2014; 202: 532-540.
10. Inampudi P, Jacobson JA, Fessell DP, et al. Soft tissue lipomas: accuracy of sonography in diagnosis with pathologic correlation. *Radiology* 2004; 233: 763-767.
11. Kuwano Y, Ishizaki K, Watanabe R, Nanko H. Efficacy of diagnostic ultrasonography of lipomas, epidermal cysts and ganglions. *Arch Dermatol* 2009; 145: 761-764.
12. Huang C, Ko S, Huang H, et al. Epidermal cysts in the superficial soft tissue. *J Ultrasound Med* 2011; 30: 11-17.
13. Park HJ, Lee SY, Lee SM, Kim WT, Lee S, Ahn S. Strain elastography features of epidermoid tumours in superficial soft tissue: differences from other benign soft-tissue tumours and malignant tumours. *Br J Radiol* 2015; 88: 20140797.
14. Tsai WC, Chiou HJ, Chou YH, Wang HK, Chiou SY, Chang CY. Differentiation between schwannomas and neurofibromas in the extremities and superficial body: the role of high-resolution and color Doppler ultrasonography. *J Ultrasound Med* 2008; 27: 161-166.
15. Reynolds DL, Jacobson JA, Inampudi P, Jamadar DA, Ebrahim FS, Hayes CW. Sonographic characteristics of peripheral nerve sheath tumours. *Am J Roentgenol* 2004; 182: 741-744.
16. Ryu JA, Lee SH, Cha EY, Kim TY, Kim SM, Shin MJ. Sonographic differentiation between schwannomas and neurofibromas in the musculoskeletal system. *J Ultrasound Med* 2015; 34: 2253-2260.
17. Chatterjee SK. Scar endometriosis: a clinicopathologic study of 17 cases. *Obstet Gynecol* 1980; 56: 81-84.
18. Hensen JH, Van Breda Vriesman AC, Puylaert JB. Abdominal wall endometriosis: clinical presentation and imaging features with emphasis on sonography. *Am J Roentgenol* 2006; 186: 616-620.
19. Francica G. Reliable clinical and sonographic findings in the diagnosis of abdominal wall endometriosis near cesarean section scar. *World J Radiol* 2012; 4: 135-140.
20. Clarke R, Suresh P, Thomas R, Freeman S. Twinkle artefact in the ultrasound diagnosis of superficial epidermoid cysts. *Ultrasound* 2016; 2: 147-153.
21. Li S, Liu L, Lv G. Diagnostic value of strain elastography for differentiating benign and malignant soft tissue masses. *Oncol Lett* 2017; 14: 2041-2044.
22. Tavare A, Alfuraih A, Hensor E, Astrinakis E, Gupta H, Robinson P. Shear-wave elastography of benign versus malignant musculoskeletal soft-tissue masses: comparison with conventional US and MRI. *Radiology* 2019; 290: 410-417.